

## Biological and hydrodynamic regulation of the microbial food web in a periodically mixed estuary

Peter M. Eldridge<sup>1</sup>

Department of Oceanography, Texas A&M University, College Station 77843

Michael E. Sieracki<sup>2</sup>

Virginia Institute of Marine Science, College of William and Mary, Gloucester Pt. 23062

### Abstract

Abundances of chroococcoid cyanobacteria and heterotrophic bacteria in surface waters of the York River subestuary covary with spring-neap tidally induced changes in the mixed-layer depth. Abundances of their principal grazers, heterotrophic protists, however, do not oscillate. A simulation model of this system using nonlinear, density-dependent functions has been developed to replicate cycles observed in the two bacterial abundances and simulate bacterial production and protistan grazing. A Jassby-Platt equation is used to determine growth rate from the mean mixed-layer light and empirically derived growth and  $\alpha$  parameters. Changes in mixed-layer depth regulate light availability, thereby controlling cyanobacterial growth rates. The model predicts a close coupling between cyanobacterial growth and grazing during destratified periods when cyanobacterial stocks are low. During stratified periods, when cyanobacteria biomass values are high, the model suggests that grazing is saturated and has little effect on cyanobacterial biomass. Grazing on heterotrophic bacteria is rarely saturated and is only loosely coupled to heterotrophic bacteria production during destratification. The model was tested at several grazer feeding preferences for cyanobacteria or heterotrophic bacteria and reproduced observed microbial biomass values most accurately when there was no initial preference. These model dynamics suggest that the heterotrophic protists fed equally well on both heterotrophic bacteria and cyanobacteria.

The elucidation of pathways in the microbial food web has produced a greater understanding of trophodynamic relationships in planktonic ecosystems (Azam et al. 1983). The role of heterotrophic protists as regulators of primary production by grazing is important to the functioning marine ecosystem (Fenchel 1987). Heterotrophic protists have been shown to be primary grazers of heterotrophic bacteria and small phytoplankton, including cyanobacteria (Landry et al. 1984; Campbell and Carpenter 1986; Sanders et al. 1989). Because heterotrophic protists oxidize a considerable portion of the total bacterial biomass, they are

also important regenerators of nutrients (Azam et al. 1983; Goldman et al. 1987a). The heterotrophic protists may also provide a large portion of the dissolved organic matter (DOM) for heterotrophic bacterial growth through excretion and cell lysis (Hagström et al. 1988).

Previous studies of material flows within the microbial food web have typically assumed steady state conditions and ignored physical forcing functions such as salinity, wind, and tides (Fenchel 1988). These abiotic factors have been shown to affect both primary production (Haas 1977) and secondary production (Ducklow 1982) in the microbial food web. The purpose of this study is to incorporate the effects of spring-neap, tidally induced stratification and destratification (S/D) cycles into a carbon model of the microbial food web in the York River, Virginia, a subestuary of Chesapeake Bay. Particular emphasis has been placed on the role of heterotrophic protists in the trophodynamic regulation of bacterial prey stocks.

The predictable spring-neap cycling of S/D in the lower York River has been well described (Haas 1977; Hayward et al. 1982, 1986). Both heterotrophic bacterial (Ray unpubl. data) and cyanobacterial abundances (Ray et al. 1989) vary in phase with S/D events.

<sup>1</sup> Current address: Department of Oceanography, Dalhousie University, Halifax, Nova Scotia B3H 4J1.

<sup>2</sup> Current address: Bigelow Laboratory for Ocean Sciences, McKown Pt. Rd., W. Boothbay Harbor, Maine 04575.

### Acknowledgments

We are indebted to Robert Ray for the thesis research that led to a description of picoplankton dynamics in the York River. We thank L. W. Haas, K. L. Webb, H. Neckles, H. W. Ducklow, and an anonymous reviewer for discussions, criticisms, and preliminary reviews of the manuscript.

This work was supported by ONR contract N00014 87-K0005 and U.S. DOE grant DE-FG05-85-ER60341.

Abundance of heterotrophic protists, on the other hand, does not change with S/D events (Ray unpubl. data). This behavior was unexpected, since these protists graze on both cyanobacteria and heterotrophic bacteria and are considered to be closely coupled to prey populations (Johnson et al. 1982; Anderson and Fenchel 1985).

Phycocyanin-rich (PC) *Synechococcus* cells dominate the York River cyanobacterial assemblage (Ray et al. 1989). These PC-rich cyanobacteria do not have the efficient light-gathering capability of the phycoerythrin-rich cyanobacteria, and thus are more likely to be light limited (Glover 1985). During summer S/D cycles, the cyanobacterial growth rate and, thereby, production rate, is controlled by average light in the mixed layer (Ray et al. 1989); the production of heterotrophic bacteria is controlled by the release rate of DOM by phototrophic and heterotrophic protists (Hagström et al. 1988). The difference between cell production and loss determines the abundance of bacteria and cyanobacteria in the mixed layer.

Our food-web model focuses on the role of heterotrophic flagellates in controlling production and loss of the picoplankton stocks during S/D events. We simulated the effect of feeding preferences of heterotrophic protists (for either cyanobacteria or heterotrophic bacteria) on population density and material flows in the microbial food web. The model shows how preference for one food item over another affects production and grazing. It also shows how protistan grazing affects the cycles in abundance of cyanobacteria and heterotrophic bacteria and how the heterotrophic protists maintain relatively constant biomass during S/D cycling.

#### The model

Our model builds on concepts developed by Ray et al. (1989) which related cyanobacterial abundance in the surface mixed layer to stratification and destratification events in the York River. Their model explained cyanobacterial abundances based on increased production during stratification and on dilution during destratification. Our model extends these results and focuses on production and grazing processes of the microbial food web. Stocks of dissolved organic carbon ( $X_1$ ), heterotrophic

Table 1. Derivation of cell carbon contents for the major stocks in the model.

	Mean cell biovolume ( $\mu\text{m}^3 \text{ cell}^{-1}$ )	C conversion ( $\text{pg C } \mu\text{m}^{-3}$ )	Cell C content ( $\text{pg C cell}^{-1}$ )
Cyanobacteria	—	—	0.115*
Bacteria	—	0.56†	0.043
Hnano	36.0‡	0.22§	7.92

\* See Ray et al. 1989.

† Bratbak 1985.

‡ Measured by image-analyzed fluorescence microscopy, Sieracki et al. 1989.

§ Børsheim and Bratbak 1987.

bacteria ( $X_2$ ), cyanobacteria ( $X_3$ ), and heterotrophic nanoplankton ( $X_4$ ) were modeled with the cell carbon contents shown in Table 1. Our model has two major parts: physical forcing functions due to the neap-spring S/D cycle and carbon flows in the surface mixed layer of the microbial food web (Fig. 1).

*Stratification and destratification*—The S/D cycle was modeled as the salinity difference between the river surface and bottom, which was simulated as the top half of a sine wave,

$$\delta s = d \sin\left(\frac{2\pi t}{\lambda}\right), \quad (1)$$

which had a wavelength ( $\lambda$ ) of 28 d and an amplitude ( $d$ ) of 5‰. Salinity difference was used with an empirically derived equation for the York River (Hayward et al. 1986) to predict the mixed layer depth  $h$ :

$$h = \exp(a - b\delta s^c). \quad (2)$$

Here  $a$  is 3.0666,  $b$  is 0.6064, and  $c$  is 0.6528. The changes in the surface-water depth and, subsequently, in surface-water dilution with bottom water were calculated from the derivative of mixed-layer depth ( $h'$ ) with respect to time  $t$  ( $\text{d}^{-1}$ ),

$$\begin{aligned} \frac{dh}{dt} = & bc \left[ d \sin\left(\frac{2\pi t}{\lambda}\right) \right]^{c-1} \\ & \times \left[ d \frac{2\pi t}{\lambda} \cos\left(\frac{2\pi t}{\lambda}\right) \right] \\ & \times \exp\left\{ a + b \left[ d \sin\left(\frac{2\pi t}{\lambda}\right) \right]^c \right\}. \quad (3) \end{aligned}$$

Biomass of the three biological stocks in bottom water were added to the surface mixed layer in proportion to advective and diffusive mixing during destratification. The only bio-

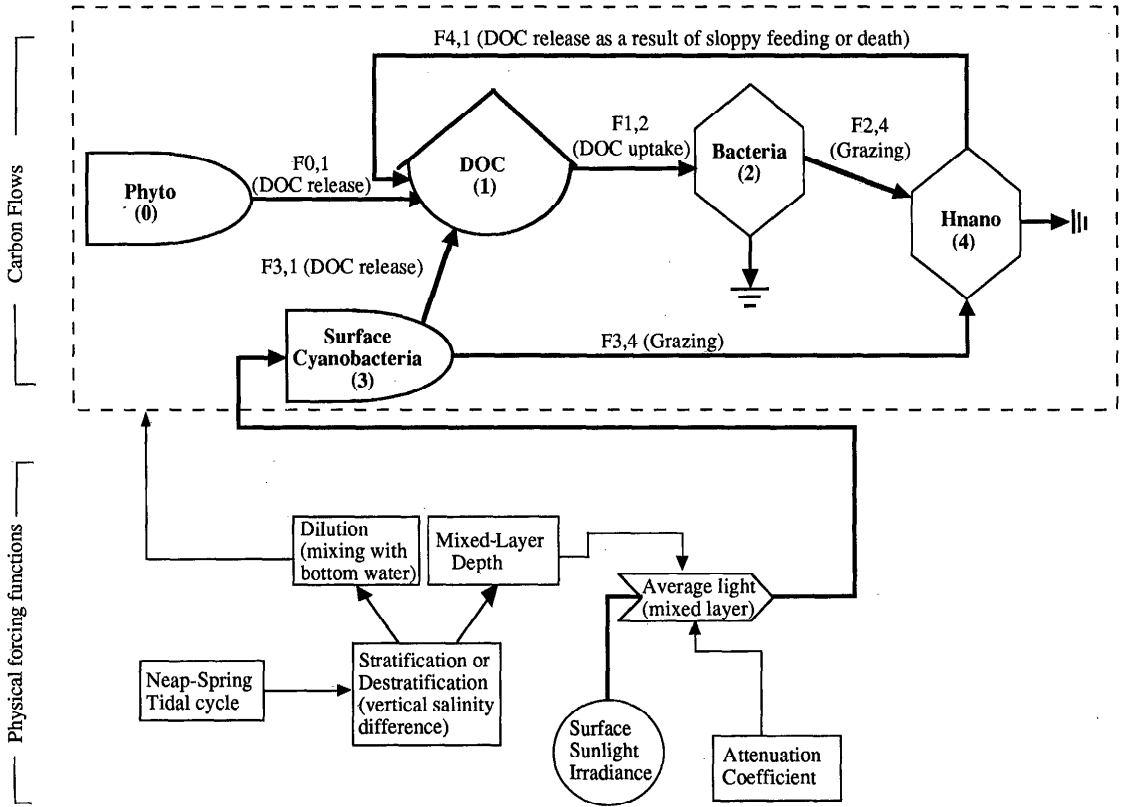


Fig. 1. General schematic outline of our model of the microbial food web in surface waters of the York River, including influences of water-column hydrodynamics. Thick lines are carbon flows or light; thin lines are informational flows.

mass changes during stratification, other than those due to losses out of the mixed layer as it became shallower, were those due to diffusive mixing. We calculated changes in mixed-layer biomass of each stock ( $D_i$ ) by modifying the Fasham et al. (1990) mixed-layer equation with a term ( $Xb_i$ ) for bottom-water biomass:

$$D_i = \left[ \frac{(m - h')(X_i - Xb_i)}{h} \right], \quad h' > 0. \quad (4)$$

Diffusive mixing ( $m$ ) (units  $m \text{ d}^{-1}$ ) between the mixed layer and bottom waters was parameterized using the same value (0.1) as in the Fasham et al. model. We set  $h'$  to 0 during stratification so that diffusive mixing was the only source of dilution to the mixed layer during this phase of the S/D cycle.

**Biological compartments**—The feeding rates and standing stocks of the biological portion of this model were based on nonlinear donor-

and recipient-controlled equations. We used the nomenclature of Christian and Wetzel (1978), in which trophic interactions were represented by resource ( $i$ ) and recipient ( $j$ ) stock pairs. In our model, these pairs consisted of either prey ( $i$ ) and predator ( $j$ ) or uptake of dissolved substrate ( $i$ ) by bacteria ( $j$ ). Four density parameters were determined for each resource and recipient pair (Christian and Wetzel 1978):  $G_{i,j}$  is the resource density below which the resource is not available as a food source (i.e. refuge level);  $A_{i,j}$  is the resource density below which uptake by the recipient is limited;  $A_j$  is the recipient density above which uptake of a resource is less than maximum (i.e. crowding);  $G_j$  is the maximum recipient density that a population can maintain when other resources are not limiting.

We assumed that the variations we saw in the three stocks during this summer experiment represented the full density range of or-

Table 2. Model parameters. The parameters below are defined in the text. All parameters are based on data from Ray et al. (1989) unless otherwise noted. Resource and recipient stocks are referred to respectively as  $i$  and  $j$  stocks. Biomass stocks are expressed in  $\mu\text{g C ml}^{-1}$ . Cell concentration for each stock can be calculated by dividing by the carbon per cell values in Table 1.

$G_{3,4} = 4,600$	Refuge level of cyanobacteria
$G_{2,4} = 98,000$	Refuge level of bacteria
$G_{1,2} = 70,000$	Refuge level of DOC set at 10% of initial value
$A_{3,4} = 40,590$	60% of max observed cyanobacteria
$A_{2,4} = 212,153$	60% of max observed bacteria
$A_{1,2} = 700,000$	Initial DOC
$A_{3,3} = 54,120$	80% of max observed cyanobacteria
$A_{2,2} = 282,871$	80% of max observed bacteria
$A_{4,4} = 25,890$	80% of the range of Hnano
$G_{3,3} = 67,653$	Max maintainable density of cyanobacteria
$G_{2,2} = 353,590$	Max observed bacteria concentration
$G_{4,4} = 32,470$	Max attained density of Hnano
$Xb_2 = 300,000$	Observed bottom-water heterotrophic bacteria concn
$Xb_3 = 11,500$	Observed bottom-water cyanobacteria concn
$Xb_4 = 19,800$	Observed bottom-water Hnano concn

ganisms in the York River; the low represented a refuge value of the organisms, and the high represented their maximum density attainable under conditions that year (Table 2). Maximum specific rates ( $\mu_{\max_j}$  or  $t_i$ ) ( $\text{d}^{-1}$ ) were obtained from the literature (Table 3). The density-dependent parameters were combined to create resource- $fb_{i,j}$  and recipient-controlled  $fb_j$  feedbacks that dampen flows of material (i.e. carbon) between each resource-recipient pair (Christian and Wetzel 1978; Wiegert and Wetzel 1979):

$$fb_{i,j} = 1 - \frac{X_i - G_{i,j}}{A_{i,j} - G_{i,j}}, \quad (5)$$

and

$$fb_j = \frac{X_j - A_j}{G_j - A_j}. \quad (6)$$

The feedbacks were dimensionless and constrained between 0 and 1, with 1 indicating maximum feedback control.

Other factors that dampened the flow of carbon from a particular prey to predator were a dimensionless metabolic correction factor and, in some cases, the presence of an alternate prey stock. The metabolic correction factor ( $C_j$ ) accounted only for carbon respiration and is simply the specific rate of respiration ( $\text{d}^{-1}$ ),  $R_j$ , divided by  $\mu_{\max_j}$ .  $C_j$  was incorporated into the combined feedback structure ( $TF_{i,j}$ ), which includes the effects of both the resource and the

recipient stocks (Eq. 7). By including  $C_j$  in the feedback, carbon will continue to move through the recipient compartment at a basal respiration rate even when growth is constrained by density or resource limitation:

$$TF_{i,j} = 1 - (1 - fb_{i,j})[1 - fb_j(1 - C_j)]. \quad (7)$$

*Cyanobacteria equations*—The cyanobacteria differential equation (Eq. 8) was formulated as production and losses through excretion ( $Ex$ ), grazing ( $Gr$ ), and mixing ( $D$ ). We did not include a photorespiration loss for cyanobacteria because this loss is small and not a source of nutrition for other model compartments:

$$\frac{dX_3}{dt} = \mu X_3(1 - fb_3) - Gr_{3,4} - Ex_{3,4} - D_3, \quad (8)$$

$$h' > 0.$$

Ray et al. (1989) showed that in the turbid York River cyanobacterial growth was a function of available light. Therefore, rather than include terms for nutrient-controlled growth in the model, we formulated cyanobacterial production as a function of light. Average light ( $I_m$ ) in the surface mixed layer was determined from incident light ( $I_0$ ), mixed layer depth ( $h$ ), and a seasonal average of the light attenuation coefficient ( $k$ ) of  $1.1 \text{ m}^{-1}$  (Ray et al. 1989):

$$I_m = I_0 \frac{1 - \exp(-kh)}{kh}. \quad (9)$$

Table 3. Parameter sensitivity. Model was run at  $\pm 1/2$  of the standard case value of each parameter listed. Changes in the model are measured as normalized root-mean-squared difference (N-RMSD) for each biological stock in the model and the experimental data. The autotrophic index (auto) and a normalized autotrophic ratio (norm) are given as a whole-model measure of difference.

Parameter (p)	Std. case	Parameter min/max	N-RMSD			Ratio	
			bact	cyano	Hnano	auto	norm
Bact (pg C cell <sup>-1</sup> )	0.043	0.02	-0.27	-0.15	0.00	0.21	-0.11
		0.06	0.18	-0.01	0.00	0.19	-0.13
Cyano (pg cell <sup>-1</sup> )	0.115	0.06	-0.24	-0.02	0.16	0.19	0.07
		0.17	0.20	-0.04	0.03	0.18	-0.25
Hnano (pg C cell <sup>-1</sup> )	7.920	3.96	-0.18	0.03	-0.03	0.18	0.24
		11.88	0.21	-0.05	0.04	0.18	-0.23
Bact, $\mu_{\max 2}$ * (d <sup>-1</sup> )	6.000	3.00	-0.21	0.05	-0.04	0.18	0.23
		9.00	0.21	-0.05	0.04	0.18	-0.23
Cyano, $\mu_{\max 3}$ * (d <sup>-1</sup> )	6.000	3.00	-0.20	0.09	-0.04	0.17	0.30
		9.00	0.21	-0.05	0.04	0.18	-0.22
Hnano, $\mu_{\max 4}$ † (d <sup>-1</sup> )	6.000	3.00	-2.03	-1.76	-0.09	0.21	-0.08
		9.00	0.09	0.16	0.01	0.17	-0.30
Phyto exudate‡ (d <sup>-1</sup> )	0.070	0.04	-0.26	-0.19	0.11	0.18	0.22
		0.11	0.00	0.13	0.04	0.16	-0.39
Hnano loss, $G_4$ § (d <sup>-1</sup> )	0.400	0.20	-0.01	-0.10	-0.07	0.16	0.38
		0.60	-0.01	0.15	0.01	0.16	-0.40
Bact respiration, $tr_2$    (d <sup>-1</sup> )	0.5	0.25	-0.09	-0.15	-0.02	0.16	0.43
		0.75	-0.05	0.15	0.01	0.16	-0.39
Hnano respiration, $tr_4$ ¶ (d <sup>-1</sup> )	0.400	0.20	-0.74	0.05	-0.27	0.17	0.34
		0.60	0.19	0.11	-0.14	0.17	-0.28
Cyano excretion, $te_3$ ‡ (d <sup>-1</sup> )	0.050	0.04	-0.20	-0.11	0.14	0.18	0.25
		0.11	0.19	0.12	-0.13	0.17	-0.30
Hnano excretion, $te_4$ # (d <sup>-1</sup> )	0.300	0.15	-0.08	-0.21	0.04	0.17	0.33
		0.45	2.22	2.24	2.01	0.22	0.14
Init. slope P vs. I, $\alpha^{**}$	0.011	0.01	-2.21	-2.02	-2.01	0.20	0.05
		0.02	2.22	2.31	2.01	0.22	0.18
Diffusive mixing, $m$ †† (m d <sup>-1</sup> )	0.100	0.05	-2.22	-2.31	-2.03	0.22	-0.18
		0.15	2.23	2.30	1.99	0.22	0.17

\* Max bacteria growth rate estimated as  $\sim 1/2$  growth rate of *Vibrio marinus* in culture, Doetsch and Cook 1973.

† Max Hnano growth rate, Fenchel 1987.

‡ Avg exudate in an estuary, Lignell 1990.

§ Proportion of total output of protozoan going to detritus and macrozooplankton, a middle value from food-web inverse analyses, Jackson and Eldridge 1992.

|| Bacterial metabolic correction term, arbitrarily set at 50% of flow (range 30–70%, Goldman et al. 1987b).

¶ Hnano respiration, set at 40% of flow (range 30–50%, Fenchel 1987).

# A middle value, Hagström et al. 1988.

\*\*  $\alpha$  in d<sup>-1</sup>  $\mu$ Einst<sup>-1</sup> m<sup>-2</sup> s<sup>-1</sup>, Ray et al. 1989.

†† Fasham et al. 1990.

Cyanobacterial growth rates,  $\mu$ (d<sup>-1</sup>), were estimated from the Jassby and Platt (1976) growth equation, using  $I_m$  and experimentally derived values for  $\alpha$  and  $\mu_{\max 3}$ (Ray et al. 1989):

$$\mu = \mu_{\max 3} \tan h \frac{\alpha I_m}{\mu_{\max 3}} \quad (10)$$

Because biomass of cyanobacteria was constrained to a similar maximum value during each stratification event, we included a concentration cap for this stock in the form of a recipient feedback (Eq. 8).

No consistent functional relationship exists between production and exudate release (Baines and Pace 1991). Therefore, we for-

mulated exudate production in the simplest way, by assuming that a fraction ( $te_3$ ) of cyanobacterial carbon per day is released as dissolved organic carbon (DOC) (Table 3).

*Phototrophic nanoplankton*—Biomass of phototrophic nanoplankton was an order of magnitude greater than the cyanobacterial biomass and was not correlated with the S/D cycle (Ray et al. 1989). This model has no compartment for phototrophic nanoplankton, which was modeled simply as a source of DOC available as a bacterial substrate. We formulated exudate from this source as a constant fraction ( $te_3$ ) of 10 times the average York River cyanobacterial biomass per day.

**Bacteria equation**—The bacteria equation (Eq. 11) was similar to that of the cyanobacteria, but included a respiration term and did not have an excretion term. We assumed that since bacteria take up DOC, any losses would be accounted for in the assimilation term:

$$\frac{dX_2}{dt} = P_2 - R_2 - G_{2,4} - D_2, \quad h' > 0. \quad (11)$$

Bacterial production ( $P_2$ ) is a function of both DOC concentration and bacterial biomass. We combined the substrate and density dependence in a total feedback term as  $TF_{1,2}$ , as shown in Eq. 12:

$$P_2 = \mu_{\max 2} X_2 (1 - TF_{1,2}). \quad (12)$$

Carbon losses from bacteria resulted from respiration and heterotrophic nanoplankton (Hnano) grazing. Respiration by bacteria was modeled in two parts: basal metabolic respiration and respiration proportional to consumption. To constrain this stock within the biomass range specified by the four density-dependent parameters required that basal respiration from the bacteria balanced the gain that resulted from the metabolic correction factor. Thus, basal respiration, the first term in Eq. 13, was a function of the size of the bacterial compartment and the recipient-controlled feedback.

$$R_2 = tr_2 X_2 fb_2 + 0.3P_2. \quad (13)$$

**Heterotrophic nanoplankton equation**—In this model, Hnano was allowed to feed simultaneously on bacteria and cyanobacteria.  $P_{2,4}$  and  $P_{3,4}$  represent the production terms resulting from feeding on these two compartments, and  $R_4$  and  $G_4$  represent losses due to respiration and predation. We assumed that Hnano could not swim fast enough to overcome the effects of dilution during destratification; therefore, a mixing term was included in the formulation of Eq. 14:

$$\frac{dX_4}{dt} = P_{2,4} + P_{3,4} - R_4 - G_4 - D_4, \quad h' > 0. \quad (14)$$

**Preferences**—When multiple resource stocks were grazed by a single predator, we used feeding preferences to calculate the consumption of each resource. No information was available from the literature about the relative prefer-

ences of Hnano for cyanobacteria and bacteria in estuaries. However, model results were sensitive to our choice of the preference value when the feeding preference was used directly. We therefore used a dynamic preference (Eq. 15) that is dependent on the relative biomass of the food resources (Fasham et al. 1990):

$$p' = \frac{p_i f(X_i)}{\sum p_i f(X_i)} \quad (15)$$

where  $p$  is the assigned preference and  $p'$  the weighted preference.

The production equation (Eq. 16) for Hnano feeding on bacteria ( $P_{2,4}$ ) and cyanobacteria ( $P_{3,4}$ ) contained both the total feedback,  $TF_{i,4}$  (Eq. 7), and the weighted preference,  $p'$  (Eq. 15):

$$P_{i,4} = p'_{i,4} \mu_{\max 4} X_4 (1 - TF_{i,4}), \quad (16)$$

which allowed the Hnano in the model to respond to a bias in selection, to biomass of prey, and to spatial constraints.

The weighted preference was formulated so that if two prey populations were not limiting, then both flows were determined only by the rate coefficients and the preference values. However, if either of the prey became limiting ( $fb_{2,4}$  or  $fb_{3,4} > 0$ ), the weighted preference for the nonlimiting resource increased (Wiegert and Wetzel 1979). It was done by setting  $f(X_j) = p(1 - fb_{i,j})$  for the  $i$  and  $j$  populations in Eq. 15. The final form of our preference equation is

$$p'_{i,4} = \frac{p_{i,4}(1 - fb_{i,4})}{p_{2,4}(1 - fb_{2,4}) + p_{3,4}(1 - fb_{3,4})}. \quad (17)$$

By using donor-controlled feedbacks (Eq. 5) in both the total feedback (Eq. 7) and the weighted preference (Eq. 17), the properties of refuge and substrate limitation in each predator-prey pair were preserved. The production equation (Eq. 16) that incorporated both these terms was, therefore, internally consistent.

Fasham et al. (1990, figure 18) showed theoretical contours of total grazing rate as a function of two prey densities, using Eq. 15 for the case of  $f(X_j) = X_j$ . A comparison of their figure with our formulation (Fig. 2) shows little difference except when one prey is nearly non-existent and the other is relatively plentiful. At these extremes, our total grazing is higher than in the model of Fasham et al. Because of

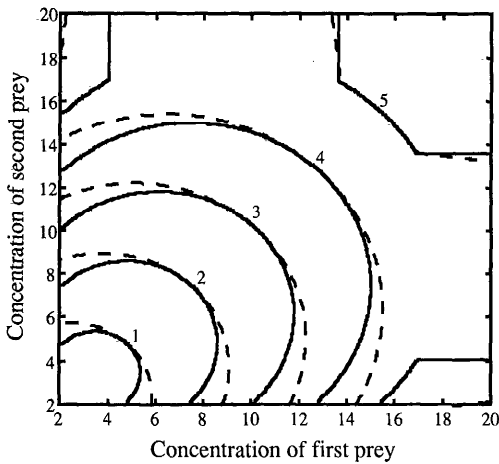


Fig. 2. Comparison of weighted preferences with formulations of Fasham et al. 1990 (---) and Wiegert and Wetzel 1979 (—). Units are arbitrary concentration units and contours are grazing in concentration  $d^{-1}$ .

the radical differences in cyanobacterial production during the S/D cycle, extremes in grazing do occur. The higher grazing pressure from our weighted preference reduced cyanobacterial biomass more rapidly than did the formulation of Fasham et al. The model generally fit observed bacterial and cyanobacterial abundances with either of the formulations when appropriate preferences were used.

*Parameterizing the model*—The carbon per cell and rate constants used in the model were chosen from the literature. These constants were derived from both laboratory experimentation and field measurements at many locations and were often reported as a range of values. Within these ranges of literature values, we chose optimum constant values by successively running the model and observing how well the results matched the York River observations. The importance of the parameters used in the model to the model's performance was tested by independently reducing and increasing each parameter by half of its value in individual runs of the model (Table 3). The effect these changes had on individual parameters was calculated with both a whole system measure of performance (the autotrophic ratio) and a measure of goodness of fit (the RMSD between each biological compartment and the York River time series data). Because the ratio of autotrophs to heterotrophs varied during the S/D cycle, we used an integrated form of

the autotrophic ratio, calculated with the trapezoidal method (Eq. 18). We formulated our autotrophic ratio so that it would vary between 0 and 1, where 0 indicates a completely heterotrophic community and 1 an uncontaminated cyanobacterial community:

$$A(p) = \frac{X_3}{X_2 + X_3 + X_4} \quad (18)$$

A sensitivity index  $S(A)$  was then calculated (Eq. 19) to measure the change in RMSD or autotrophic ratio  $A(p)$  relative to change in parameter  $p$ . We made both of our sensitivity indices nondimensional by normalizing measurement  $A$  and parameter  $p$  by its value in the standard case,  $A_s$  and  $p_s$ :

$$S(A) = \frac{A(p) - A_s}{A_s} \times \left( \frac{p - p_s}{p_s} \right)^{-1} \quad (19)$$

For an  $S(A)$  of 1, there is one-to-one correspondence in the change in model performance,  $A(p)$ , and the change in each parameter,  $p$  (Fasham et al. 1990).

Parameters that affected the fit of the data to the model did not necessarily affect the normalized autotrophic ratio. The model fit to data was especially sensitive to the Hnano excretion rate, the initial slope of the  $P$  to  $I$  curve, and the diffusive mixing constant. Changes in these factors cascaded through the food web, affecting all the components equally (Table 3). As a result, there was no relative difference that would change the normalized autotrophic index. On the other hand, changes in the bacterial and Hnano respiration parameters affected the heterotrophic components of the food web, but not the autotrophic compartments, and were reflected in the normalized autotrophic index. Thus, within the domain of the parameters tested, those parameters that dealt with rates of the cyanobacteria growth and those with recycling potential affected the dynamics of the whole microbial system, while parameters such as respiration and loss rate of Hnano by death from metazoan grazing had no effect on other compartments of the food web. Carbon content per cell of the cyanobacteria, bacteria, and Hnano had only small effects on the sensitivity parameters.

There were no high values of normalized sensitivity parameters, indicating an absence

of discontinuities in the parameter space of the model (Table 3). Generally, a 50% change in a parameter resulted in a change of <50% in the normalized sensitivity parameters, suggesting that the model is well posed. The RMSD of the standard case was <50% of the mean, showing that the model was also accurate.

We were initially concerned that the maximum biomass of Hnano in the York River,  $G_4$ , was not the maximum attainable. Resources for Hnano were plentiful during the stratification period, but grazing by macrozooplankton, not considered in this model, could have caused some reduction in the biomass of Hnano. However, changing the Hnano loss rate over a range of 0.2–0.6 had negligible effects on the RMSD of any biological stock (Table 3). These results suggest that either the model is robust against this type of departure from the density-dependent assumption or that  $G_4$  actually was the maximum sustainable biomass of Hnano.

We did not include the density parameters in our sensitivity test because their value is set by abundance data. We did change these parameters in separate runs to see, in a general way, how they affected the performance of the model. The parameter that changed flux rates  $A_{i,j}$  and  $A_j$  was sequentially increased, while the parameters that affected the maximum and minimum limits of the stocks ( $G_{i,j}$  and  $G_j$ ) were fixed. We noted little difference in the total integrated flux of carbon through the model during these simulations. Stock abundances, however, oscillated through a greater range as  $A_j$  values were increased.

The model was stable over simulation time periods of up to 1,000 d. In general, the model preserves the important functional relationships of size, trophic interaction, and specificity. It was written with Matlab and run on a DECstation 5000/250.

### Results and discussion

The model predictions were consistent with physical and biological observations in the river (Fig. 3). The predicted cyanobacterial biomass increased to  $65 \mu\text{g C liter}^{-1}$  during stratification and decreased during destratification to  $15 \mu\text{g C liter}^{-1}$ . Observed biomass of carbon varied over a similar range in two of the three S/D events. A major deviation between the predicted salinity difference between the river

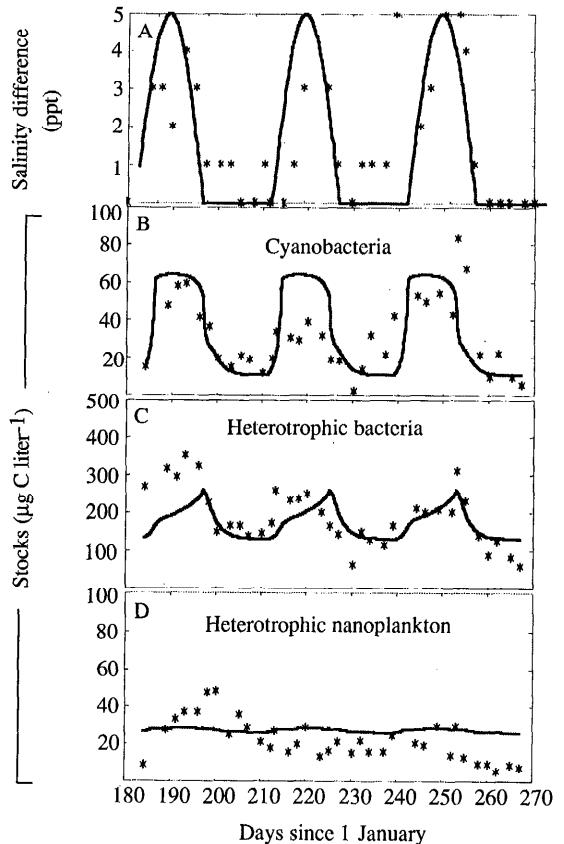


Fig. 3. Comparison of model prediction (—) and observed data (\*) from Ray et al. 1989. Top-to-bottom salinity difference (A), cyanobacteria (B), heterotrophic bacteria (C), and heterotrophic nanoplankton (D) in surface waters of the lower York River with the initial cyanobacteria: bacteria feeding preference ratio set at 0.5:0.5.

surface and bottom and observed data occurred before the third stratification period in late summer (near day 240 of that year). This unpredicted stratification coincided with a significant pulse of freshwater runoff in the river (U.S. Geol. Surv. 1987). A concomitant early increase in cyanobacteria and heterotrophic bacteria occurred with this event and continued through the predicted stratification period (Fig. 3). There was also an initial increase in Hnano biomass during the first stratification period not simulated by the model. As discussed above, maximum Hnano biomass ( $G_4$ ) may be due in part to macrozooplankton grazing instead of density-dependent constraints. The trend in Hnano biomass during the first

Table 4. Recipient-controlled and resource-controlled feedbacks dampen carbon flow to microbial stocks. Feedbacks have values between 0 and 1. Increasing values of a feedback restricts flow to a compartment, with a value of 1 turning the flow off.

Stocks	Conditions	
	Stratified	Destratified
Cyanobacteria		
Recipient controlled	0.45	0.00
Bacteria		
Recipient controlled	0.00	0.00
Resource controlled	0.95	0.91
Hnano		
Recipient controlled	0.25	0.19
Cyanobacteria resource controlled	0.00	0.42
Bacteria resource controlled	0.00	0.10

stratification could, therefore, be the result of a temporary release from grazing pressure.

*Biomass under feedback control*—Hydrodynamic control of cyanobacterial biomass, acting through feeding relationships, shaped trends in biomass of heterotrophic components of microbial food webs in phase with the spring-neap tidal cycle (Fig. 3). Cyanobacterial growth was limited by light, as the mixed-layer depth extended to 15 m during destratified periods. During stratified periods, higher average light in the shallow mixed layer stimulated cyanobacteria growth. We did not have DOC data from the York River, but we assumed that DOC released through phytoplankton and microbial food-web processes was quickly used by the heterotrophic bacteria (Hagström et al. 1988). Calculated DOC release rates were low relative to the size of the bacterial stock supported by the DOC. As a result, the bacteria were always resource limited (Table 4). Biomass of Hnano was recipient controlled during stratified periods and resource controlled during mixed periods when prey stocks were low. The source of the high Hnano recipient-controlled feedback may actually be metazoan grazing not accounted for in the model.

*Multiple resource models*—In successive model runs, we tested the full range of possible feeding preferences for bacteria and cyanobacteria to see how well they fit observations (Fig. 4). Changes in the preference values had little effect on prey abundance, except in the extreme cases where preferences for the two stocks were set  $<0.1$  or  $>0.7$ . Within this range the RMSD (units,  $\mu\text{g C liter}^{-1}$ ) of the three bio-

logical compartments was between 50 and 70% of the in situ biomass means. When the feeding preference for bacteria or cyanobacteria was low ( $<0.1$ ), the RMSD between in situ and model biomass increased. The better fit of the data to the model under intermediate preference conditions showed that grazing on both bacteria and cyanobacteria is required to explain trends in the data from the York River.

*Single-resource models*—We have demonstrated that the goodness of fit of the multiple-resource model explains biomass trends better than single-resource models. However, we do not know if this resulted from a difference in scaling or from differences in trends in species abundance. Setting the preference for one prey item to 0 and the other to 1 resulted in a single-prey resource for the Hnano predator. These single-resource food chains could occur if either heterotrophic bacteria or cyanobacteria proved refractory to digestion or were not within the feeding size range of the predator (Fenchel 1987; Fuhrman et al. 1989). Bacteria were the prey in our first single-resource model (Fig. 5A). In this model there was a small increase in bacteria biomass in response to an influx of bottom-water bacteria into the mixed layer late in the stratified period. Biomass of Hnano increased slightly in response to the higher bacterial biomass.

When cyanobacteria were the only prey in the single-resource model, biomass of Hnano and cyanobacteria alternated between a production-dominated phase during stratification, in which biomass of the two stocks was high, and a typical Lotka-Volterra predator-

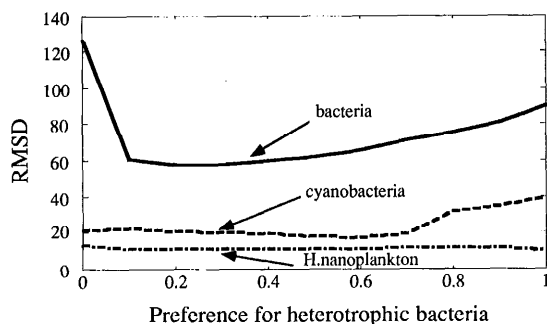


Fig. 4. Numerical experiment in which the model was run at feeding preferences increasing in steps of 0.1 for bacteria. The preference for cyanobacteria was decremented so the combined preference was always 1. RMSD (units,  $\mu\text{g C liter}^{-1}$ ) between model results and York River observations were calculated for each iteration of the model run and plotted with cubic spline fits.

prey cycle during destratification (Fig. 5B). In the production-dominated phase, the high cyanobacterial production supported Hnano predation without a reduction in the biomass of cyanobacteria. Consequently, maximum biomass of both cyanobacteria and Hnano co-occur. During destratification, when production was low, grazing reduced cyanobacterial biomass, generating a typical predator-prey cycle in which Hnano and cyanobacterial peaks were out of phase.

In each of the single-resource models, the bacterial or cyanobacterial compartment not used as a resource remained uniformly high during the S/D cycle (Fig. 5A, B). As a single prey, bacteria and cyanobacteria followed the same trend of increasing biomass during stratification as they did in the multiple-prey model, except their biomasses were lower. The Hnano in the multiple-prey model (Fig. 5C) remained constant, consistent with the York River time series data. However, in the single-prey model, there was not always sufficient prey to sustain the high biomass of Hnano, causing the predator density to vary with the S/D cycle.

*Hydrodynamic regulation of the microbial food web*—We have accounted for variations in the three biological stocks in this model based on patterns in cyanobacterial production and feeding relationships. How much of the dynamics of the food web is related to changes in mixed-layer depth? We know that if biomass of a biological stock remains con-

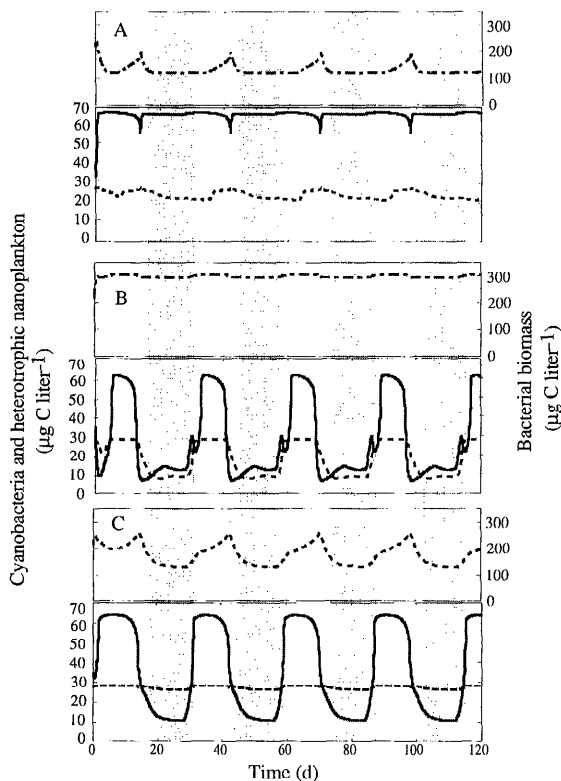


Fig. 5. Comparison of multiple- and single-resource models. A. Bacteria : cyanobacteria preference set at 1 : 0. B. Preference set at 0 : 1. C. Preference set at 0.5 : 0.5. Concentrations in mixed layer of bacteria (— · —), cyanobacteria (—), and Hnano (---). Shaded areas are destratified periods.

stant, the integrated biomass in the mixed layer must follow the profile described by mixed-layer depth over the S/D cycle (Fig. 6A). To keep cell biomass constant as the mixed layer deepens, the combination of production and addition of biota from the bottom water must balance advection and diffusion into the mixed layer.

Two of the biological stocks, bacteria and Hnano, have trends in depth-integrated mixed-layer biomass that are similar to the mixed-layer depth profile (Fig. 6B, C). Because the biomass of bacteria changed during the S/D cycle, its integrated biomass profile also diverged slightly from the mixed-layer profile. In the case of bacteria, bottom-water biomass was high ( $300 \mu\text{g C liter}^{-1}$ ) and little additional growth was required to maintain biomass (Table 5). The bottom-water biomass of Hnano

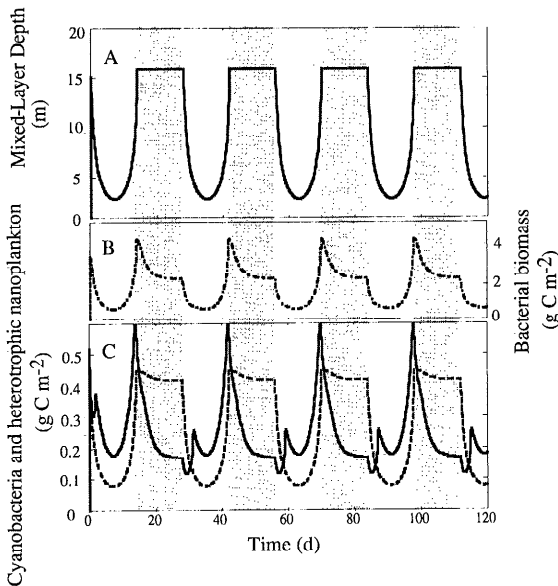


Fig. 6. As Fig. 5, but depth-integrated carbon in the mixed layer. A. Mixed-layer depth. B. Bacteria biomass. C. Cyanobacteria and Hnano.

was not as high as the surface-water biomass. The deficit in bottom-water Hnano biomass entering the surface mixed layer was compensated for by a high Hnano growth rate during the transition between stratification and destratification. We had only a few samples in which bottom-water Hnano were counted, so

Table 5. Effect of stratification and destratification on excretion, gross growth efficiency, respiration, and growth rate. Percent excretion shows the contribution of phytoplankton, cyanobacteria, and Hnano to total DOC flux.

	Stratification	Destratification
Excretion of DOC (%)		
Phytoplankton	42	69
Cyanobacteria	6	3
Hnano (recycled)	52	28
Growth efficiency (%)		
Bacteria	30	30
Hnano	42	60
Respiration ( $\mu\text{g C ml}^{-1}$ )		
Bacteria	21	15
Hnano	70	20
Growth rate ( $\text{d}^{-1}$ )		
Cyanobacteria	1.5–3.0	1.2
Bacteria	0.2	0.3
Hnano	4.0	1.8–2.0

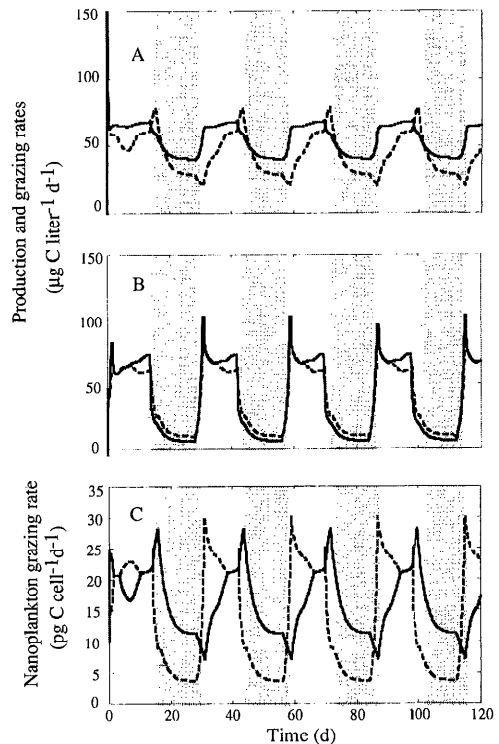


Fig. 7. Simulations of production and grazing in the microbial food web. A. Bacterial production (—) and Hnano grazing (---) on bacteria. B. Cyanobacteria production (—) and Hnano grazing (---) on cyanobacteria. C. Cell-specific grazing rates of Hnano on bacteria (—) and cyanobacteria (---). Shaded areas are destratified periods.

we cannot be sure of how well the model represents dilution of the Hnano compartment. The model predicts that a pulse in Hnano production will balance the effect of bottom-water dilution, keeping Hnano biomass constant.

Integrated cyanobacterial biomass did not follow patterns in mixed-layer depth, but instead had a maximum integrated biomass in the transition between stratification and destratification events (Fig. 6C). This high integrated cyanobacterial biomass was caused by both an injection of bottom-water cyanobacteria and a high production rate. The production rate was not sustained as mixed-layer depth increased. Grazing rapidly depleted the integrated cyanobacterial biomass as the river became destratified. The integrated cyanobacteria biomass remained low until stratification began (Fig. 7A, B).

The model shows that increased production at the onset of stratification did not initially result in greater cyanobacterial biomass (Fig. 7B). Because the microbial predator had growth rates similar to that of the cyanobacteria, most of the production was consumed by Hnana. Only after bacterial production and cyanobacterial production overwhelmed the predator with prey, thereby saturating grazing, did the biomass of cyanobacteria increase.

The concept of saturated grazing at high prey densities is not new. Gallegos (1989) used the dilution method to show examples of saturated feeding kinetics. Grazing was saturated in our model at cyanobacterial abundances between  $2.5$  and  $4.0 \times 10^5$  cells  $\text{ml}^{-1}$  or 28 and 46  $\mu\text{g C liter}^{-1}$ . The growth rate for cyanobacteria in the model ranged from  $0.48 \text{ d}^{-1}$  during destratification to  $1.00 \text{ d}^{-1}$  during stratification. During stratification, growth and grazing were the same ( $0.48 \text{ d}^{-1}$ ), with grazing ranging up to a maximum value of  $0.65 \text{ d}^{-1}$  during stratification before becoming saturated. These values are within the range of cyanobacterial growth and grazing noted by others (Landry et al. 1984; Campbell and Carpenter 1986).

There have been estimates of saturating grazing greater than those shown in our model. Metabolic inhibitor experiments have provided several estimates of grazing  $>0.65 \text{ d}^{-1}$ , including one as high as  $0.83 \text{ d}^{-1}$  (Campbell and Carpenter 1986). Our low grazing rates may be the result of the relatively high cyanobacterial abundances (high consumption but low turnover of cyanobacteria biomass by grazing) and the fact that the protozoan grazers were themselves grazed in our model. Gallegos (1989) showed that grazing by organisms at higher trophic levels may result in substantial reductions in the apparent growth rates of phytoplankton and, consequently, in grazing.

*Heterotrophic bacterial production and grazing*—There is a growing consensus that grazing and heterotrophic bacterial net production are balanced in steady state marine and freshwater systems (Sanders et al. 1989). When they are not, factors such as sinking, cell death, and viruses are thought to cause the difference (Sanders et al. 1989). Our model suggests that Hnana, by switching prey resources, may cause heterotrophic bacterial production to be underused. Annual cycles of stratification and destratification may lead to close coupling of

growth and consumption of heterotrophic bacteria, but short-term perturbations, such as the S/D cycle, lead to a disequilibrium between production and consumption. Instead of the close coupling seen in the cyanobacteria stock (except during saturated grazing), there was only a weak covariance between heterotrophic bacterial net production and grazing in our model. During the stratification and destratification events, bacterial production was 30 and  $60 \mu\text{g C liter}^{-1} \text{ d}^{-1}$ , respectively. The grazing rate was generally 10–20% below bacterial production (Fig. 7A). A review of the literature by Sanders et al. (1989) showed similar results from several production and grazing experiments in marine systems. The average of the dilution experiments of Landry et al. (1984) and Ducklow and Hill (1985), using our carbon per cell value and converting to consistent units, yields  $71 \mu\text{g C liter}^{-1} \text{ d}^{-1}$  production and  $44 \mu\text{g C liter}^{-1} \text{ d}^{-1}$  grazing. This model did not include the effects of allochthonous inputs of DOC, which could modify the heterotrophic bacteria production rates (Findlay et al. 1991).

*The effect of consumption by heterotrophic nanoplankton on microbial prey stocks*—To determine the relative impact of the Hnana predator on cyanobacteria and bacteria, we examined cell-specific grazing rates. The Hnana cell-specific consumption of bacteria exceeded that of cyanobacteria during destratified periods and equaled that of cyanobacteria during stratified periods (Fig. 7C). These dynamics were a logical consequence both of the increased abundance of the bacterial and cyanobacterial stocks during stratification and of Hnana dependency on the heterotrophic bacterial stock during destratification. By increasing consumption at the same time cyanobacterial production declined, Hnana played an important role in shaping the trends in cyanobacterial abundance.

*Density-dependent interactions between production and grazing*—S/D events and other physical forcing events are known to affect phytoplankton community dynamics. The importance of these events in structuring grazing and growth processes is less well understood. As has been shown in this model and by experiments (Goldman et al. 1987a), components of the microbial food web react to environmental stresses on short time scales because of their small size and their high rates

of growth and consumption. In our model, changes in feedback, caused by density-dependent processes, dampen population oscillations, similar to the way that growth and grazing can rapidly adjust to trophic level imbalances.

The model gives us a mechanism to explore the way a predator can affect prey populations. In our model, Hnano grazing was found to affect cyanobacterial production. By continually removing biomass from the prey stocks, grazing maintained the prey stock density below the maximum maintainable density. During the stratified period, this produced resource and spatial conditions that promoted high growth rates for both Hnano and cyanobacteria (Table 5). In the model, these dynamics were reflected in a low resource-controlled feedback for Hnano (0.0) and a low recipient-controlled feedback for cyanobacteria (0.45) (Table 4). Hnano grazing also stimulated bacterial production by returning about a third of the grazed carbon to the microbial loop as DOM through excretion and lysis.

The changes in production and grazing rates caused reciprocal changes in gross growth efficiency and respiration of the three trophic species (Table 5). Much of the difference in these rates during stratification and destratification was caused by the changing proportions of basal to total respiration during fluctuations in abundance and production. The predicted values of bacterial and Hnano gross growth efficiency varied within the ranges reported in several laboratory studies (Fenchel 1987; Goldman et al. 1987b). The differences in the growth rate, respiration, and excretion shown by the model during stratification and destratification suggest a linkage between hydrodynamic processes and food-web processes that can affect not only growth and grazing rates, but the whole physiology of the organisms.

## References

- ANDERSEN, P., AND T. FENCHEL. 1985. Bacterivory by microheterotrophic flagellates in seawater samples. *Limnol. Oceanogr.* **30**: 198-202.
- AZAM, F., AND OTHERS. 1983. The ecological role of water-column microbes in the sea. *Mar. Ecol. Prog. Ser.* **10**: 257-263.
- BAINES, S. B., AND M. L. PACE. 1991. The production of dissolved organic matter by phytoplankton and its importance to bacteria: Patterns across marine and freshwater systems. *Limnol. Oceanogr.* **36**: 1078-1090.
- BRATBAK, G. 1985. Bacterial biovolume and biomass estimations. *Appl. Environ. Microbiol.* **49**: 1488-1493.
- BØRSHEIM, K. Y., AND G. C. BRATBAK. 1987. Cell volume to cell carbon conversion factors for a bacterivorous *Monas* sp. enriched from seawater. *Mar. Ecol. Prog. Ser.* **36**: 171-175.
- CAMPBELL, L., AND E. J. CARPENTER. 1986. Estimating the grazing pressure of heterotrophic nanoplankton on *Synechococcus* spp. using the sea water dilution and selective inhibitor techniques. *Mar. Ecol. Prog. Ser.* **33**: 121-129.
- CHRISTIAN, R. R., AND R. L. WETZEL. 1978. Interaction between substrate, microbes, and consumers of *Spartina* detritus in estuaries, p. 93-113. *In* M. L. Wiley [ed.], *Estuarine interactions*. Academic.
- DOETSCH, R. N., AND T. M. COOK. 1973. *Introduction to bacteria and their ecology*, 1st ed. University Park.
- DUCKLOW, H. W. 1982. Chesapeake Bay nutrient and plankton dynamics. I. Bacterial biomass and production during spring tidal destratification in the York River, Virginia, estuary. *Limnol. Oceanogr.* **27**: 651-659.
- , AND S. M. HILL. 1985. Tritiated thymidine incorporation and the growth of heterotrophic bacteria in warm core rings. *Limnol. Oceanogr.* **30**: 260-272.
- FASHAM, M. J. R., H. W. DUCKLOW, AND S. M. MCKELVIE. 1990. A nitrogen-based model of plankton dynamics in the oceanic mixed layer. *J. Mar. Res.* **48**: 591-639.
- FENCHEL, T. 1987. Ecology of protozoa: The biology of free-living phagotrophic protists. *Sci. Technol.*
- . 1988. Marine plankton food chains. *Annu. Rev. Ecol. Syst.* **19**: 19-38.
- FINDLAY, S., AND OTHERS. 1991. Weak coupling of bacterial and algal production in a heterotrophic ecosystem: The Hudson River estuary. *Limnol. Oceanogr.* **36**: 268-278.
- FUHRMAN, J. A., T. D. SLEETER, C. A. CARLSON, AND L. M. PROCTOR. 1989. Dominance of bacterial biomass in the Sargasso Sea and its ecological implications. *Mar. Ecol. Prog. Ser.* **57**: 207-217.
- GALLEGOS, C. L. 1989. Microzooplankton grazing on phytoplankton in the Rhode River, Maryland: Non-linear feeding. *Mar. Ecol. Prog. Ser.* **57**: 23-33.
- GLOVER, H. E. 1985. The physiology and ecology of the marine cyanobacterial genus *Synechococcus*, p. 49-107. *In* *Advances in aquatic microbiology*, V. 3. Academic.
- GOLDMAN, J. C., D. A. CARON, AND M. R. DENNETT. 1987a. Nutrient cycling in a microflagellate food chain: 4. Phytoplankton-microflagellate interactions. *Mar. Ecol. Prog. Ser.* **38**: 75-87.
- , ———, AND ———. 1987b. Regulation of gross growth efficiency and ammonium regulation in bacteria by substrate C:N ratio. *Limnol. Oceanogr.* **32**: 1239-1252.
- HAAS, L. W. 1977. The effect of the spring-neap tidal cycle on the vertical salinity structure of the James, York and Rappahannock Rivers in Virginia, U.S.A. *Estuarine Coastal Mar. Sci.* **5**: 485-496.
- HAGSTRÖM, A., F. AZAM, A. ANDERSSON, J. WIKNER, AND F. RASSOULZADEGAN. 1988. Microbial loop in an oligotrophic pelagic marine ecosystem: Possible roles of cyanobacteria and nanoflagellates in the organic fluxes. *Mar. Ecol. Prog. Ser.* **49**: 171-178.

- HAYWARD, D., L. W. HAAS, J. D. BOON, K. L. WEBB, AND K. D. FRIEDLAND. 1986. Empirical models of stratification variations in the York River estuary, Virginia, USA, p. 346-367. *In* Tidal mixing and plankton dynamics. Coastal Estuarine Stud. V. 17. Springer.
- , C. S. WELCH, AND L. W. HAAS. 1982. York River destratification: An estuary-subestuary interaction. *Science* **216**: 1413-1414.
- JACKSON, G. A., AND P. M. ELDRIDGE. 1992. Foodweb analysis of a planktonic system off southern California. *Prog. Oceanogr.* **30**: 233-251.
- JASSBY, A. D., AND T. PLATT. 1976. Mathematical formulation of the relationship between photosynthesis and light for phytoplankton. *Limnol. Oceanogr.* **21**: 540-547.
- JOHNSON, P. W., H. XU, AND J. M. SIEBURTH. 1982. The utilization of chroococcoid cyanobacteria by marine protozooplankters but not by calanoid copepods. *Ann. Inst. Oceanoogr. Paris* **58**: 297-308.
- LANDRY, M. R., L. W. HAAS, AND V. L. FAGERNESS. 1984. Dynamics of microbial plankton communities: Experiment in Kancohe Bay, Hawaii. *Mar. Ecol. Prog. Ser.* **16**: 127-133.
- LIGNELL, R. 1990. Excretion of organic carbon by phytoplankton: Its relation to algal biomass, primary productivity and bacterial secondary productivity in the Baltic Sea. *Mar. Ecol. Prog. Ser.* **68**: 85-99.
- RAY, R. T., L. W. HAAS, AND M. E. SIERACKI. 1989. Autotrophic picoplankton dynamics in a Chesapeake Bay sub-estuary. *Mar. Ecol. Prog. Ser.* **52**: 273-285.
- SANDERS, R. W., K. G. PORTER, S. J. BENNETT, AND A. E. DEBIASE. 1989. Seasonal patterns of bacterivory by flagellates, ciliated rotifers, and cladocerans in a freshwater plankton community. *Limnol. Oceanogr.* **34**: 673-687.
- SIERACKI, M. E., S. W. REICHENBACH, AND K. L. WEBB. 1989. Evaluation of automated threshold selection methods for accurately sizing microscopic fluorescent cells by image analysis. *Appl. Environ. Microbiol.* **55**: 2762-2772.
- U.S. GEOLOGICAL SURVEY. 1987. Water resources data—Virginia: Water Year 1986. Water Resour. Div.
- WIEGERT, R. G., AND R. L. WETZEL. 1979. Simulation experiments with a 14-compartment salt marsh model, p. 7-39. *In* R. F. Dame [ed.], Marsh-estuarine systems simulation. Univ. So. Carolina.

*Submitted: 12 August 1991*

*Accepted: 8 December 1992*

*Revised: 3 March 1993*